high imperfection. (In reflection topographs, imperfect regions will always produce stronger *integrated* reflections than perfect regions and will also do so in transmission topographs under low-absorption conditions.) The island B is assumed to be as perfect as C, but is slightly misoriented with respect to C. The topograph images sketched in (b)–(e) could represent either reflection topographs or transmission topographs from a specimen thin compared with the dimension CD in Fig. 2.7.1.2. [Possible distortion of the images relative to the shape of (a) is neglected: this matter is considered later.] First, suppose that continuous radiation is emitted from the source S. If the ratio b/a is quite small, the topograph image will resemble (b). The island A is detected by diffraction contrast whereas island B will not show any area contrast since by assumption the incident radiation contains wavelengths enabling B to satisfy the Bragg condition just as well as C. The low-angle B–C boundary may show up, however, since it contains dislocations that will produce diffraction contrast and might be individually resolvable with a high-resolution topographic technique. Orientation contrast of B becomes manifest when b is increased, and measurement of the misorientation is then possible from the displacement of the image of B [as shown in (c)] consequent upon the different direction of Bragg-reflected rays issuing from it compared with those from C.

Next, suppose that S emits a limited range of wavelengths, *e.g.* characteristic $K\alpha$ radiation, and let the incident beam be collimated to have an angular spread in the plane of incidence that is smaller than the component in that plane of the misorientation between B and C, but larger than the angular range of reflection of C or A. Then, if the specimen is rotated about the ω axis so that A and C satisfy the Bragg condition, B will not do so and the topograph will resemble (d). [Island A shows up in (d) by diffraction contrast, as in (b).]. Appropriate rotation of the specimen will bring B into the Bragg-reflecting orientation, but will eliminate reflection from A and C, as shown in (e). The images (d) and (e) will not undergo significant change with variation in the ratio b/a, except for loss of resolution as b/a increases. The sensitivity of misorientation measurement will increase as the angular and wavelength spread of the incident beam are reduced, but when the angular range of a monochromatic incident beam is lowered to a value comparable with the angular range of reflection of the perfect crystal (generally only a few seconds of arc), it will not be possible with one angular setting alone to obtain an image that will distinguish between diffraction contrast and orientation contrast in the clear way shown in (d). The distinction will require comparison of a series of topographs obtained during a step-wise sweep of the angular range of reflection by the specimen. This is the procedure adopted in double-crystal or multicrystal topography, as described in Sections 2.7.3 and Subsection 2.7.4.2.

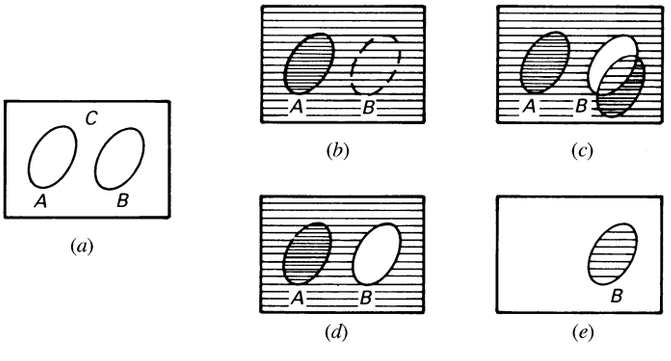

Fig. 2.7.1.3. Differentiation between orientation contrast and diffraction contrast in types of topograph images, (b)–(e), of a crystal surface (a).

Details concerning diverse variants in diffraction geometry used in X-ray topographic experiments, treatments of the diffraction contrast theory underlying X-ray topographic imaging of lattice defects, and listings of applications of X-ray topography can be found in reviews and monographs of which a selection follows. All aspects of X-ray topography are covered in the survey edited by Tanner & Bowen (1980). Armstrong & Wu (1973), Tanner (1976), and Lang (1978) describe experimental techniques and review their applications. The dynamical-diffraction theoretical basis of X-ray topography is emphasized by Authier (1970, 1977). Kato (1974) and Pinsker (1978) deal comprehensively with X-ray dynamical diffraction theory, which is also the topic of Part 5 of *IT* B (1996). Introductions to this theory have been presented by Batterman & Cole (1964), Hart (1971), and Hildebrandt (1982), the latter two being especially relevant to X-ray topography.

2.7.2. Single-crystal techniques

2.7.2.1. *Reflection topographs*

Combining the simple diffraction geometry of Fig. 2.7.1.1 with a laboratory microfocus source of continuous radiation offers a simple yet sensitive technique for mapping misorientation textures of large single crystals (Schulz, 1954). One laboratory X-ray source much used produces an apparent size of S 30 μm in the axial direction and 3 μm in the plane of incidence. Smaller source sizes can be achieved with X-ray tubes employing magnetic focusing of the electron beam. Then b/a ratios between $\frac{1}{2}$ and 1 can be adopted without serious loss of geometric resolution, and, with $a = 0.3$ m typically, misorientation angles of $10''$ can be measured on images of the type (c) in Fig. 2.7.1.3. The technique is most informative when the crystal is divided into well defined subgrains separated by low-angle boundaries, as is often the case with annealed melt-grown crystals. On the other hand, when continuous lattice curvature is present, as is usually the case in all but the simplest cases of plastic deformation, it is difficult to separate the relative contributions of orientation contrast and diffraction contrast on topographs taken by this method. In principle, the separation could be effected by recording a series of exposures with a wide range of values of b, and it becomes practicable to do so when exposures can be brief, as they can be with synchrotron-radiation sources (see Section 2.7.4.).

For easier separation of orientation contrast and diffraction contrast, and for quicker exposures with conventional X-ray sources, collimated characteristic radiation is used, as in the Berg–Barrett method. Barrett (1945) improved an arrangement earlier described by Berg (1931) by using fine-grain photographic emulsion and by minimizing the ratio b/a, and achieved high topographic resolution (~ 1 μm). The method was further developed by Newkirk (1958, 1959). A typical Berg–Barrett arrangement is sketched in Fig. 2.7.2.1. Usually, the source S is

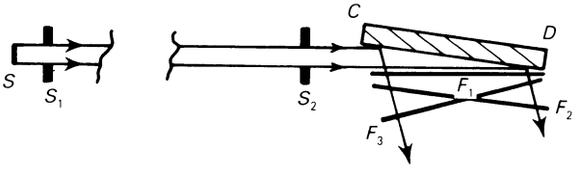

Fig. 2.7.2.1. Berg–Barrett arrangement for surface-reflection topographs.

the focal spot of a standard X-ray tube, giving an apparent source 1 mm square perpendicular to the incident beam. The openings of the slits S_1 and S_2 are also 1 mm in the plane of incidence, and the distance S_1–S_2 (which may be identified with the distance a) is typically 0.3 m. The specimen is oriented so as to Bragg reflect asymmetrically, as shown. Softer radiations, *e.g.* Cu $K\alpha$, Co $K\alpha$ or Cr $K\alpha$, are employed and higher-angle Bragg reflections are chosen ($2\theta_B \simeq 90^\circ$ is most convenient). Fig. 2.7.2.1 indicates three possible film orientations, F_1–F_3. (These possibilities apply in most X-ray topographic arrangements.) Choice of orientation is made from the following considerations. If minimum distance b is required over the whole length CD, then position F_1 is most appropriate. If a geometrically undistorted image of CD is needed, then position F_2, in which the film plane is parallel to the specimen surface, satisfies this condition. If a thick emulsion is used, it should receive X-rays at normal incidence, and be in orientation F_3. If high-resolution spectroscopic photographic plates are used, in which the emulsion thickness is $\sim 1\,\mu$m only, then considerable obliquity of incidence of the X-rays is tolerable. But these plates have low X-ray absorption efficiency. Nuclear emulsions (particularly Ilford type L4) are much used in X-ray topographic work. Ilford L4 is a high-density emulsion (halide weight fraction 83%) and hence has high X-ray stopping power. The usual minimum emulsion thickness is 25 µm. Such emulsions should be oriented not more than about 2° off perpendicularity to the X-ray beam if resolution loss due to oblique incidence is not to exceed 1 µm (with correspondingly closer limits on obliquity for thicker emulsions). With 1 mm openings of S_1 and S_2, and $a = 0.3$ m, most of the irradiated area of CD will receive an angular range of illumination sufficient to allow both components of the $K\alpha$ doublet to Bragg reflect. In these circumstances, the distance b must be everywhere less than 1–2 mm if image spreading due to superimposition of the α_1 and α_2 images is not to exceed a few micrometres. In order to eliminate this major cause of resolution loss (and, incidentally, gain sensitivity in misorientation measurements), the apertures S_1 and S_2 should be narrowed and/or a increased so that the angular range of incidence on the specimen is less than the difference in Bragg angle of the α_1 and α_2 components for the particular radiation and Bragg angle being used. (This condition applies equally in the transmission specimen techniques, described below.). With a narrower beam, the illuminated length of CD is reduced. This disadvantage may be overcome by mounting the specimen and film together on a linear traverse mechanism so that during the exposure all the length of CD of interest is scanned. In this way, surface-reflection X-ray topographs can be recorded for comparison with, say, etch patterns or cathodoluminescence patterns (Lang, 1974).

2.7.2.2. *Transmission topographs*

The term 'X-ray topograph' was introduced by Ramachandran (1944) who took transmission topographs of cleavage plates of diamond using essentially the arrangement shown in Fig. 2.7.1.2. (In this case, S was a 0.3 mm diameter pinhole placed in front of the window of a W-target X-ray tube so as to form a point source of diverging continuous radiation.) Ramachandran adopted a distance $a = 0.3$ m and ratio a/b of about 12, which produced images of about 25 µm geometrical resolution having the characteristics of Fig. 2.7.1.3(*b*), *i.e.* sensitive to diffraction contrast but not to orientation contrast. For each reflection under study, the film was inclined to the incident beam with that obliquity calculated to produce an undistorted image of the specimen plate. Guinier & Tennevin (1949) studied both diffraction contrast and orientation contrast in continuous-radiation transmission topograph images. Their minimum b/a ratio was set by the need to avoid overlap of Laue images of the crystal produced by different Bragg planes.

Collimated characteristic radiation is used in the methods of 'section topographs' (Lang, 1957) and 'projection topographs' (Lang, 1959*a*), the latter being sometimes called 'traverse topographs'. Fig. 2.7.2.2 explains both techniques. When taking a section topograph, the specimen CD, usually plate shaped, is stationary (disregard the double-headed arrow in the figure). The ribbon-shaped incident beam issuing from the slit P is Bragg reflected by planes normal, or not far from normal, to the major surfaces of the specimen. As drawn, the Bragg planes make an angle α with the normal to the X-ray entrance surface of the specimen, the positive sense of α being taken in the same sense as the deviation $2\theta_B$ of the Bragg-reflected rays. If the crystal is sufficiently perfect for multiple scattering to occur within it (with or without loss of coherence), then the multiply scattered rays associated with the Bragg reflection excited will fill the volume of the triangular prism whose base is ORT, the 'energy-flow triangle' or 'Borrmann triangle', contained between OT and OR whose directions are parallel to the incident wavevector, $\mathbf{K}_0$, and diffracted wavevector, $\mathbf{K}_h$, respectively. Both the $\mathbf{K}_0$ and $\mathbf{K}_h$ beams issuing from the X-ray exit surface of the crystal carry information about the lattice defects within the crystal. However, it is usual to record only the $\mathbf{K}_h$ beam. This falls on the film, F, in a strip extending normal to the plane of incidence, of height equal to the illuminated height of the specimen multiplied by the axial magnification factor $(a + b)/a$, and forms the section topograph image. The screen, Q, prevents the $\mathbf{K}_0$ beam from blackening the film but has a slot allowing the diffracted beam to fall on F. A diffraction-contrast-producing lattice defect cut by OT at I will generate supplementary rays parallel to $\mathbf{K}_h$ and will produce an identifiable image on F at I', the 'direct image' or 'kinematic image' of the defect. The depth of I within CD can be found *via* the measurement of $I'T'/R'T'$. From a series of section topographs taken with a known translation of the specimen between each topograph, a three-dimensional construction of the trajectory of defect I (*e.g.* a dislocation line) within the crystal can be built up. To obtain good definition of the spatial width of the ribbon incident beam cutting the crystal, the distance between P and the crystal is kept small. The minimum practicable opening of P is about 10 µm. If diffraction is occurring from planes perpendicular to the X-ray entrance surface of the specimen, *i.e. symmetrical Laue case* diffraction, the width $R'T'$ of the section topograph image is simply $2t \sin\theta_B$, t being the specimen thickness, and neglecting the contribution from the

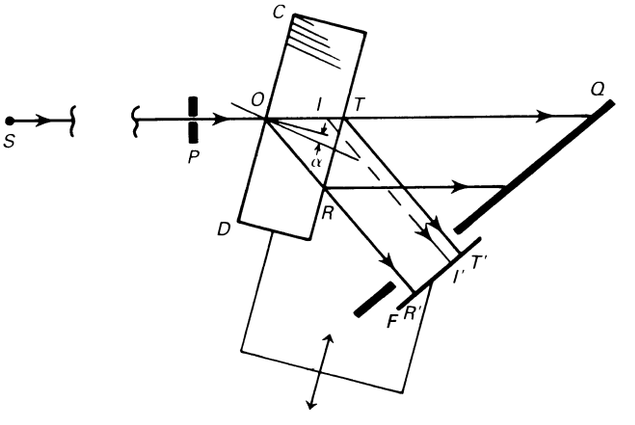

Fig. 2.7.2.2. Arrangements for section topographs and projection topographs.

references